Investigation of electromagnetically induced transparency in the strong probe regime

S. Wielandy* and Alexander L. Gaeta
School of Applied and Engineering Physics, Cornell University, Ithaca, New York 14853
(Received 15 December 1997)

We study the response of an inhomogeneously broadened atomic three-level ladder system to a strong probe beam under conditions in which electromagnetically induced transparency would be induced on a weak probe beam. Theoretical analysis and experimental data show that saturation effects associated with the strong probe can substantially alter the behavior of the system and can result in enhanced probe absorption under exactly the same circumstances in which a weak probe would experience enhanced transparency. Strong probe effects are also shown to lead to a breakdown of the correspondence between population inversion and gain. A power-series solution of the density-matrix equations describing the ladder system provides a physical picture for strong probe effects in terms of interfering multiphoton transition pathways. [S1050-2947(98)06609-8]

PACS number(s): 42.50.Gy, 42.50.Hz

I. INTRODUCTION

Phenomena associated with electromagnetically induced transparency (EIT) have attracted considerable attention in recent years and offer a variety of interesting and potentially important applications [1]. The essence of EIT is that an atomic coherence is induced in a multilevel system by a strong ''control'' laser field, which alters the response of the system to a ''probe'' laser field. Although systems in which both control and probe fields are strong have been studied previously, the emphasis was understanding the evolution and propagation of laser pulses [2]. Previous studies of EIT systems in the steady state with cw lasers have focused primarily on the weak-probe limit. Since many of the potential applications of EIT [3–6] are to enhance or facilitate nonlinear processes in which the probe beam is not necessarily weak, it is important to understand the effect of a strong probe field on the EIT process. An early investigation of atomic coherences in a homogeneously broadened three-level system was performed in the pioneering work of Whitley and Stroud [7], in which they made several interesting observations that foreshadowed many of the results of later work on EIT. They demonstrated the modification of the system's absorption profile for a strong probe field due to a strong control field and showed that it was possible to achieve a steady-state population inversion that did not result in optical gain. However, their analysis did not focus attention on the change in the response of their system as the strength of the probe field is increased.

In this work, we consider the closed three-level ladder scheme shown in Fig. 1, which is experimentally realized by a gas of Rb atoms with the energy levels as shown. The $|2\rangle \rightarrow |3\rangle$ transition is driven by a control laser field at frequency ω_c, and the $|1\rangle \rightarrow |2\rangle$ transition is driven by a probe laser field at ω_p, which is not necessarily weak. We present both a theoretical and experimental investigation of this Doppler-broadened system in which the cw pump and probe fields are both allowed to be strong. Our results show that saturation effects resulting from the strong probe diminish the induced transparency and can even lead to enhanced absorption under circumstances in which a weak probe would experience enhanced transmission. In Sec. II, we present a theoretical treatment, where we solve the steady-state density-matrix equations for this system and perform a Doppler average over the atomic velocity distribution. In Sec. III, we present experimental results and compare them with the predictions of the theory. In Sec. IV, we present a power-series solution of the density-matrix equations that provides a physical picture for strong-probe-field effects in terms of interfering multiphoton transition pathways. In Sec. V we offer concluding remarks.

II. THEORY

Consider the three-level ladder system shown in Fig. 1, which we assume in this model to be closed. Let ω_{21} be the frequency of the $|1\rangle \rightarrow |2\rangle$ transition, and ω_{32} be the frequency of the $|2\rangle \rightarrow |3\rangle$ transition. The system is driven by a control field with amplitude E_c at frequency ω_c, and by a probe field with amplitude E_p at frequency ω_p. Solving the density-matrix equations for this system in steady state and applying the rotating-wave approximation yields the following set of equations:

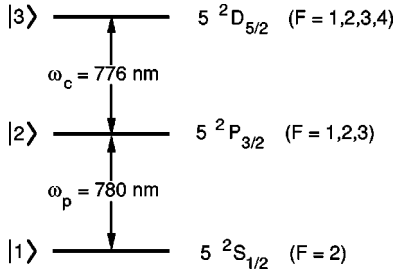

FIG. 1. Energy level scheme for the ladder system. Also shown are the corresponding states and wavelength separations for atomic rubidium.

*Department of Physics, Cornell University, Ithaca, New York 14853.

$$\rho_{21}=\frac{i/2[\Omega_p(\rho_{22}-\rho_{11})-\Omega_c^*\rho_{31}]}{\gamma_{21}-i\delta_p}, \tag{1a}$$

$$\rho_{32}=\frac{i/2[\Omega_c(\rho_{33}-\rho_{22})+\Omega_p^*\rho_{31}]}{\gamma_{32}-i\delta_c}, \tag{1b}$$

$$\rho_{31}=\frac{i/2(\Omega_p\rho_{32}-\Omega_c\rho_{21})}{\gamma_{31}-i(\delta_p+\delta_c)}, \tag{1c}$$

$$\rho_{22}=\frac{i}{2\Gamma_2}(\Omega_p^*\rho_{21}-\Omega_p\rho_{12}), \tag{1d}$$

and

$$\rho_{33}=\frac{i}{2\Gamma_3}(\Omega_c^*\rho_{32}-\Omega_c\rho_{23}), \tag{1e}$$

where $\delta_c=\omega_c-\omega_{32}$, $\delta_p=\omega_p-\omega_{21}$, $\Omega_c=2\mu_{32}E_c/\hbar$, and $\Omega_p=2\mu_{21}E_p/\hbar$. In the absence of collisions, $\gamma_{ij}=(\Gamma_i+\Gamma_j)/2$, where Γ_i is the natural decay rate of level $|i\rangle$. In the limit of a weak probe, Gea-Banacloche *et al.* [8] showed that the solution to these equations for ρ_{21} to first order in the probe field and to all orders in the control field is

$$\rho_{21}=\frac{i\Omega_p/2}{i\delta_p-\gamma_{21}+\dfrac{\Omega_c^2/4}{i(\delta_p+\delta_c)-\gamma_{31}}}, \tag{2}$$

which displays the essence of EIT. The response of the system to the probe field is determined by the above expression through the proportionality between the susceptibility and ρ_{21}, that is,

$$\chi_{21}=-\frac{2N\mu_{21}^2}{\hbar\Omega_p}\rho_{21}. \tag{3}$$

The effect of the control laser is seen in the extra term that appears in the denominator of Eq. (2). Moreover, the two-photon detuning term suggests that even in a Doppler-broadened atomic vapor it is possible to realize a system that benefits from significant two-photon Doppler cancellation by using counterpropagating control and probe lasers. The behavior of the Doppler-broadened system can be calculated by adding appropriate Doppler-detuning terms to Eq. (2) and performing a weighted average over a Maxwellian velocity distribution.

In the limit in which the probe beam is strong, the above system of equations is more complicated to solve, and the behavior of the analytic solution is less transparent. Furthermore, to make the problem tractable it is necessary to assume that the system is closed, which is not required in the weak-probe limit since in that limit there is no population transfer. Experimentally, the energy-level structure is more complex, and in particular the presence of hyperfine structure in the ground state results in possible complications caused by optical pumping effects in the presence of a strong probe field. Nonetheless, significant physical insight can be gained from our simple three-level model into the effect of driving the ladder system with probe and control fields that are both allowed to be strong.

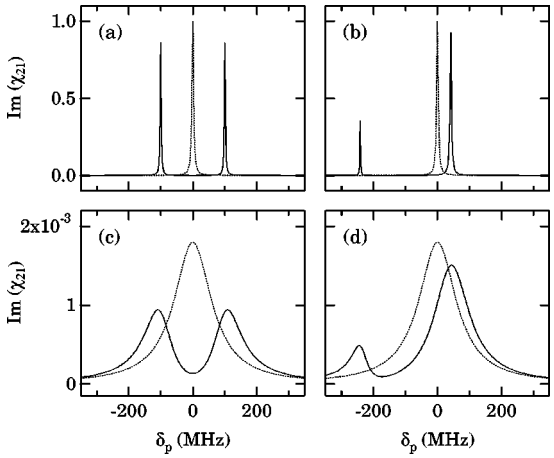

FIG. 2. Theoretically calculated, homogeneously broadened probe absorption as a function of probe detuning from resonance under different conditions. The dotted line is with the control field off, and the solid line is with the control field on. In (a) $\Omega_p=0.1$ MHz, $\Omega_c=200$ MHz, $\delta_c=0$; (b) $\Omega_p=0.1$ MHz, $\Omega_c=200$ MHz, $\delta_c=200$ MHz; (c) $\Omega_p=100$ MHz, $\Omega_c=200$ MHz, $\delta_c=0$; (d) $\Omega_p=100$ MHz, $\Omega_c=200$ MHz, $\delta_c=200$ MHz.

We calculate the response of the Doppler-broadened three-level ladder system to a strong probe field for the case of counterpropagating probe and control fields by making the substitutions

$$\delta_p\rightarrow\delta_p+\frac{v}{c}\omega_p, \tag{4a}$$

$$\delta_c\rightarrow\delta_c-\frac{v}{c}\omega_c, \tag{4b}$$

and

$$(\delta_p+\delta_c)\rightarrow(\delta_p+\delta_c)+\frac{v}{c}(\omega_p-\omega_c) \tag{4c}$$

in the density-matrix equations of Eq. (1). We then numerically solve this system of equations for ρ_{21} and perform an average of the result over a Maxwell-Boltzmann velocity distribution. To provide a connection to our experiments, calculations were performed using the parameters appropriate for the ladder system provided by the $5S_{1/2}$, $5P_{3/2}$, and $5D_{5/2}$ levels of atomic Rb, as shown in Fig. 1. The values used for the decay rates are $\Gamma_2/2\pi=6$ MHz, $\Gamma_3/2\pi=1$ MHz, and $\Gamma_1/2\pi=0$ since $|1\rangle$ is the ground state.

Although experimentally we operate in the Doppler-broadened regime, insight into the behavior of this system can nonetheless be gained by first looking at the homogeneously broadened case. Figure 2 shows a typical set of theoretically calculated, homogeneously broadened absorption profiles under a variety of conditions, and several features are worthy of note. For zero detuning of the control beam [Figs. 2(a) and 2(c)], the initial probe absorption line splits into two peaks of equal amplitude, known as an Autler-Townes doublet. In the weak probe limit [Fig. 2(a)], the peaks are separated by the Rabi frequency of the control field, but for a stronger probe field [Fig. 2(c)] the separation of the peaks increases. For nonzero control detuning, the

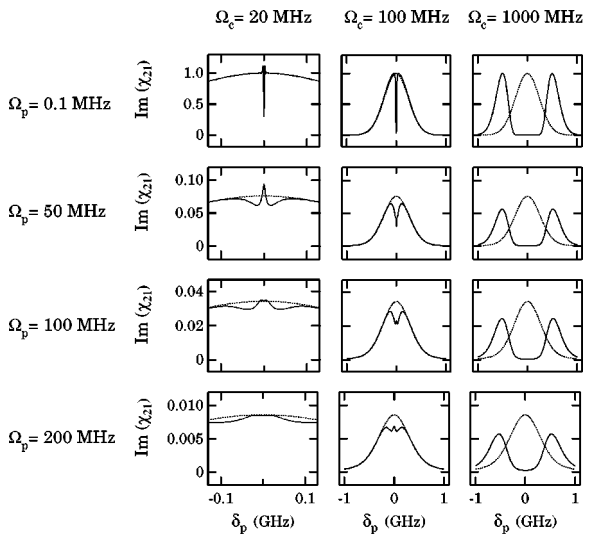

FIG. 3. Theoretically calculated, Doppler-broadened probe absorption as a function of probe detuning from resonance for several probe and control field strengths. The solid line in each figure is with the control field on, the dotted line is with the control field off. Control and probe field strengths are indicated in the column and row headings.

amplitudes of the two peaks are no longer equal and their separation is larger. In the weak probe limit [Fig. 2(b)], the separation is well described by the generalized Rabi frequency, given by

$$\Omega_c' = \sqrt{\Omega_c^2 + \delta_c^2}. \tag{5}$$

At high probe powers with $\delta_c \neq 0$ [Fig. 2(d)], the doublet spacing is again larger than in the weak probe case. These changes in the doublet spacing alter the overlap of the contributions of the different velocity subgroups to the Doppler-averaged susceptibility and have an important impact on the behavior of the inhomogeneously broadened system. As the probe power is increased, the amplitude of a particular absorption peak decreases and its width increases, displaying the expected saturation and power-broadening behavior. As illustrated in Fig. 2(a), as long as $\Omega_c \gtrsim \sqrt{\Gamma_2 \Gamma_3}$, in the weak-probe case there will be nearly zero absorption at $\delta_p = 0$. However, in the presence of significant power broadening due to a strong probe field as shown in Fig. 2(c), the broader peaks that make up the Autler-Townes doublet now overlap and contribute to significant absorption at $\delta_p = 0$. This also leads to a deterioration of EIT in the Doppler-broadened case.

Figure 3 shows calculated absorption profiles for the Doppler-averaged case for several control field and probe field strengths. At low probe powers, we reproduce previous results [8], where EIT results in a hole in the absorption profile whose width is comparable to Ω_c. In cases where Ω_c is small compared to the Doppler width of the absorption profile, $\Delta \nu_D$, this hole appears as a very narrow feature. Although the persistence of EIT in the presence of Doppler broadening for $\Omega_c < \Delta \nu_D$ is a result of the two-photon Doppler cancellation arising from counterpropagating lasers beams, Shepherd, Fulton, and Dunn [9] demonstrated the surprising result that EIT is optimized when $\omega_c > \omega_p$ rather

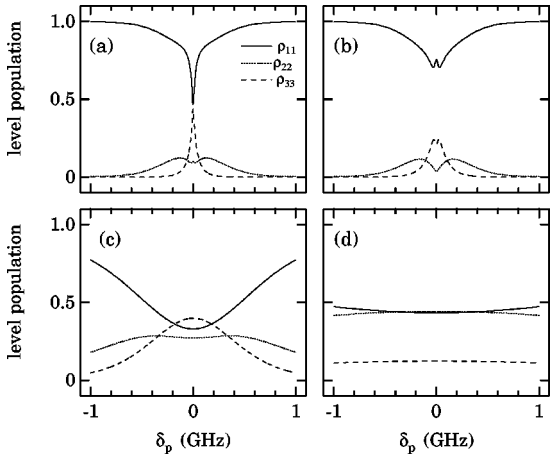

FIG. 4. Theoretically calculated, Doppler-broadened level populations for various probe and control Rabi frequencies. The solid line is ρ_{11}, the dotted line is ρ_{22}, and the dashed line is ρ_{33}. In (a) $\Omega_p = 100$ MHz, $\Omega_c = 100$ MHz; (b) $\Omega_p = 100$ MHz, $\Omega_c = 200$ MHz; (c) $\Omega_p = 1000$ MHz, $\Omega_c = 500$ MHz; (d) $\Omega_p = 5000$ MHz, $\Omega_c = 1000$ MHz.

than for the case of perfect two-photon Doppler cancellation. In cases where Ω_c significantly exceeds the Doppler width, the results qualitatively resemble the homogeneously broadened case, in which a single absorption line is split into two peaks separated by the Rabi frequency of the control laser.

Typically, under conditions in which both fields are strong but the control field is stronger than the probe field, the qualitative behavior is similar to that of the weak probe limit. However, comparing the results at a fixed control power while varying the probe power leads to a reduction in the maximum induced transparency that can be achieved. A qualitative change in behavior occurs for a relatively weak control field when the probe field is comparable to or greater in magnitude than the control field. In these cases, different spectral features appear near the line center, and atomic coherences can even give rise to enhanced absorption rather than induced transparency. This point is made clear by comparing the traces in the first column of Fig. 3 for $\Omega_c = 20$ MHz at probe strengths of $\Omega_p = 0.1$ MHz and $\Omega_p = 50$ MHz. Under identical conditions except for the strength of the probe field, there is an absorption dip in the weak probe limit at $\delta_p = 0$ that transforms into a region of enhanced absorption in the presence of a stronger probe field. In the latter case, induced transparency can be recovered by increasing the strength of the control field as shown by the traces in the last three columns of the second row of Fig. 3. The ''electromagnetically enhanced absorption'' behavior shown here is similar to behavior recently observed using pulsed lasers in molecular NO [10].

Figure 4 shows the level populations for the Doppler broadened case under a variety of conditions. Note that there are conditions under which a steady-state population inversion exists between levels $|3\rangle$ and $|2\rangle$ [Figs. 4(a), 4(b), and 4(c)] and where a small inversion exists between levels $|2\rangle$ and $|1\rangle$ [Fig. 4(d)]. Moreover, examination of the corresponding susceptibilities (not shown) reveals that these inversions are not correlated with optical gain and illustrates the breakdown of the traditional correspondence between inversion and gain. The converse effect of gain without inver-

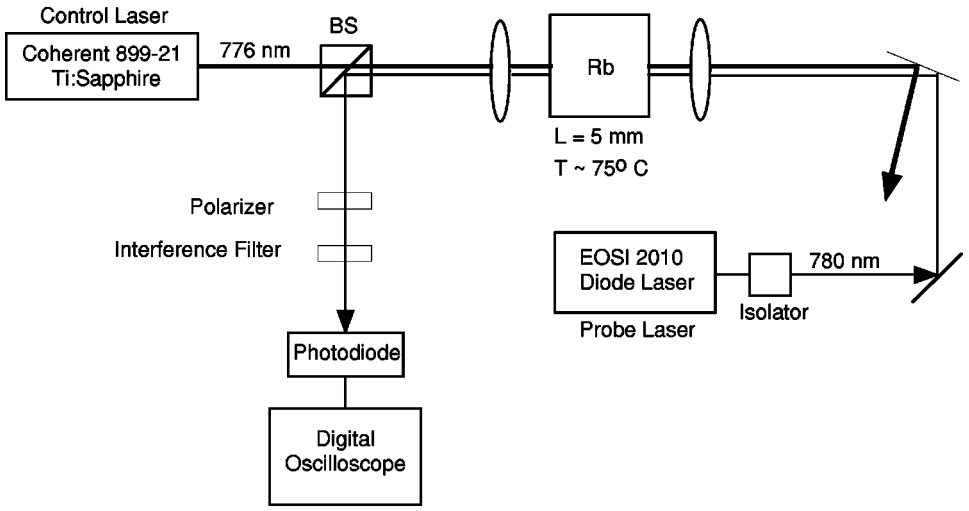

FIG. 5. Schematic of the experimental setup. Probe and control beams are counterpropagating and orthogonally polarized.

sion has led to the demonstration of an inversionless laser [11].

III. EXPERIMENTAL RESULTS

Our three-level ladder system is experimentally realized by a gas of Rb atoms. As shown in Fig. 1, the probe transition is the $5S_{1/2} \rightarrow 5P_{3/2}$ $D2$ line at a wavelength of 780 nm, and the control transition is $5P_{3/2} \rightarrow 5D_{5/2}$ at a wavelength of 776 nm. The natural linewidth of the probe transition is 6 MHz, and the natural linewidth of the control transition is 1 MHz. The geometry of the apparatus is shown in Fig. 5. The Rb vapor cell is 5 mm thick and is held at a fixed temperature between 50 °C and 100 °C by heater elements, which allows the atomic number density to be varied from approximately 10^{11} cm^{-3} to 10^{13} cm^{-3}. Doppler broadening of both the control and probe transitions in this temperature range results in linewidths for each transition of roughly 600 MHz and is the dominant broadening mechanism under these conditions. The control transition is driven by a single-frequency Ti:sapphire laser, which can produce powers in excess of 1 W at the Rb cell. The probe transition is driven by a single-frequency external-cavity diode laser. The Ti:sapphire laser beam is focused into the cell with an $f = 40$-cm lens, which can result in values for the Rabi frequency of the control beam in excess of 10 GHz. To achieve favorable overlap with the control beam, the probe beam mode is made round with an anamorphic prism pair and is focused more tightly than the control beam by an $f = 25$-cm lens. The lasers are counterpropagating and have orthogonal linear polarizations to allow for easy separation of the control and probe beams with a polarizing beamsplitter. A diffraction grating is used as one of the steering elements for the probe beam, so that Ti:sapphire light (at 776 nm rather than 780 nm) does not feed directly into the diode laser. In addition, the diode laser is protected from other optical feedback by a Faraday isolator that provides in excess of 30 dB of isolation. The probe beam is detected by a photodiode, and background light is reduced by the use of a polarizer and a 3-nm-bandwidth interference filter.

Data are taken by scanning the frequency of the diode laser and recording the detected probe transmission on a digital oscilloscope. Frequency calibration of the laser scan is obtained by using the known hyperfine splitting and isotope shifts of the Rb $5S_{1/2}$ ground state, which for the two common isotopes results in four resolvable peaks as the laser is scanned across the $D2$ line. Although the hyperfine levels of the $5P_{3/2}$ state are not resolvable as a result of their small splittings in comparison to the Doppler width, the overall linewidth is slightly in excess of what would be expected for a single Doppler-broadened line. EIT is observed for each of the four resolvable peaks, and all the data shown in this paper are associated with transitions from the $F = 2$ hyperfine level of the ^{85}Rb $5S_{1/2}$ ground state. The Rb vapor pressure is adjusted so that the transmission of the probe at the center of this line with no control field is approximately 30%. In all cases, the control laser is tuned nearly to resonance by adjusting its frequency so that EIT is optimized in the weak probe limit.

Probe transmission measurements are shown in Fig. 6. We find good qualitative agreement between experiment and

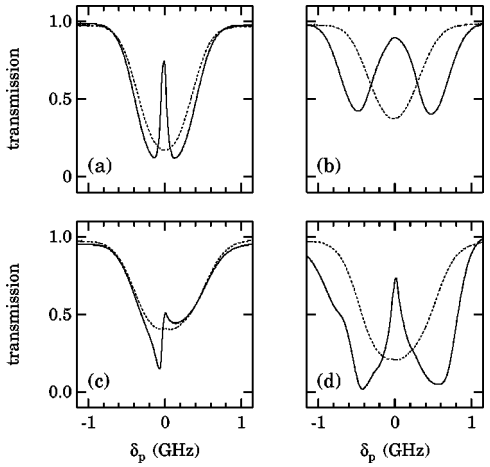

FIG. 6. Experimental probe transmission measurements for several probe strengths. The solid line is with the control field on, and the dotted line is with the control field off. In (a) $I_p = 10$ mW/cm^2, $I_c = 35$ W/cm^2; (b) $I_p = 10$ mW/cm^2, $I_c = 400$ W/cm^2; (c) $I_p = 2$ W/cm^2, $I_c = 35$ W/cm^2; (d) $I_p = 2$ W/cm^2, $I_c = 400$ W/cm^2.

theory. Under optimal conditions, the presence of the control beam causes the transmission of the weak probe beam to increase from roughly 35% to over 90%. At modest values of Ω_c, we observe EIT as a deep but narrow dip in the transmission profile [Fig. 6(a)], and at large control Rabi frequencies the probe transmission profile splits into two clearly distinct peaks separated by Ω_c [Fig. 6(b)]. As the strength of the probe is increased, the level of induced transparency is reduced, and under conditions where Ω_p becomes comparable to Ω_c, strong-probe effects are seen to lead to enhanced absorption [Fig. 6(c)]. Finally, if the probe remains strong and the strength of the control field is increased, EIT can be recovered [Fig. 6(d)].

Quantitative comparison with theory is difficult for a number of reasons. One difficulty lies in determining the effective Rabi frequency of the beams, particularly the probe. Since the probe is absorbed as it propagates through the cell, its intensity is not uniform throughout the cell. In addition, since both lasers are intense and are nearly resonant with an atomic transition, self-focusing effects may lead to a change in the spatial profile of the focused beams. Since EIT itself has been shown to have an effect on the self-focusing process [12,13], accurately determining the focused spot size of the two beams is made more complicated. The hyperfine structure associated with the intermediate $5P_{3/2}$ state and with the $5D_{5/2}$ state results in additional complications not considered in our theoretical model and makes it difficult to determine effective Rabi frequencies and field detunings. In addition, our experimental three-level system is not closed, and the presence of hyperfine structure in the ground state allows for the possibility of optical pumping effects. However, optical pumping effects would tend to increase the transmission of the probe beam as its intensity is increased, which is the opposite of what we observe experimentally, indicating that it is less important than other strong probe effects that are included in our model. Finally, the effects of the finite linewidth of both lasers are not considered in our model. Despite all of these complications, the fact that the experimental data demonstrate the principal qualitative features predicted by our theoretical model clearly indicates that it contains the most important physical mechanisms responsible for strong probe effects.

IV. DISCUSSION

Our theoretical and experimental results demonstrate that the strength of the probe field can alter the behavior of our system in important ways. In particular, increasing the probe strength decreases the degree of EIT and can result in electromagnetically enhanced absorption. To understand the underlying reason for this behavior, recall that the fundamental mechanism responsible for EIT is the quantum interference between two alternate pathways for the $|1\rangle \rightarrow |2\rangle$ transition. In the presence of the probe alone, there is the conventional one-photon pathway directly from $|1\rangle$ to $|2\rangle$ [Fig. 7(a)]. If one adds a strong control field, then an additional pathway results from the three-photon transition shown in Fig. 7(b), which entails the absorption of a single probe photon and the absorption and subsequent reemission of a control photon. In our system, the signs of the transition amplitudes associated with these two pathways are opposite, resulting in destructive interference between the two pathways and in the reduction of the total probability that a probe photon will be absorbed. If the probe field is allowed to be strong, then additional multiphoton pathways exist from $|1\rangle$ to $|2\rangle$. In particular, there is the five-photon transition shown in Fig. 7(c) involving three probe photons and two control photons. This term and other higher-order terms become important as the strength of the probe is increased and interfere with the one-photon and three-photon terms, which can result in a deterioration of the induced transparency and even in induced absorption. This ''interfering-pathways'' description is illustrated by performing an iterative solution to the system of Eqs. (1a)–(1e) for resonant probe and control fields to obtain a power series expansion for ρ_{21} that contains terms up to third order in Ω_p and Ω_c. The result is

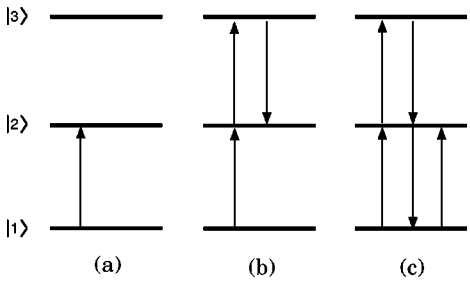

FIG. 7. Alternate quantum-mechanical pathways for the $|1\rangle \rightarrow |2\rangle$ transition.

$$\rho_{21}=\frac{-i\Omega_p}{2\gamma_{21}}\left[1-\frac{\Omega_c^2}{4\gamma_{21}\gamma_{31}}-\frac{\Omega_p^2}{\Gamma_2\gamma_{21}}+A\Omega_p^2\Omega_c^2\right], \tag{6}$$

where

$$A=\frac{1}{2\Gamma_2\gamma_{21}^2\gamma_{31}}+\frac{1}{8\Gamma_2\gamma_{21}\gamma_{31}\gamma_{32}}+\frac{1}{16\gamma_{21}\gamma_{31}^2\gamma_{32}}-\frac{1}{4\Gamma_3\Gamma_2\gamma_{21}\gamma_{32}}-\frac{1}{8\Gamma_3\gamma_{21}\gamma_{31}\gamma_{32}}. \tag{7}$$

In the absence of collisional dephasing, the last four terms in Eq. (7) cancel, and Eq. (6) reduces to

$$\rho_{21}=\frac{-i\Omega_p}{2\gamma_{21}}\left[1-\frac{\Omega_c^2}{4\gamma_{21}\gamma_{31}}-\frac{\Omega_p^2}{\Gamma_2\gamma_{21}}+\frac{\Omega_p^2\Omega_c^2}{2\Gamma_2\gamma_{21}^2\gamma_{31}}\right]. \tag{8}$$

This expression clearly shows the various multiphoton processes that contribute to the response of the ladder system when the probe and control fields are both strong. The first term in Eq. (8) represents linear absorption [Fig. 7(a)], and the second is the lowest-order term in the control field which interferes destructively with the linear absorption term and is responsible for EIT [Fig. 7(b)]. The third term is independent of the control field, and is the lowest-order term responsible for saturated absorption. Finally, the fourth term in Eq. (8) represents the five-photon process shown in Fig. 7(c), which has the same sign as the linear absorption term and therefore tends to increase the absorption of the probe field. Other higher-order terms become important for sufficiently strong probe and control fields, but the general trends indicated by both our complete numerical solution of the density-matrix

equations and by our experimental results are clearly reflected by the various terms in Eq. (8).

V. CONCLUSION

In this paper, we presented theoretical results describing EIT in a three-level ladder system without any approximations with respect to the strength of the probe field. Our predictions along with our experimental measurements show that departing from the weak-probe limit leads to a deterioration of EIT and can result in electromagnetically enhanced absorption. A power-series solution of the density-matrix equations provides a physical picture for strong probe effects in terms of interfering multiphoton transition pathways.

[1] K.-J. Boller, A. Imamoglu, and S. E. Harris, Phys. Rev. Lett. **66**, 2593 (1991).
[2] A. Kasapi, M. Jain, G. Y. Yin, and S. E. Harris, Phys. Rev. Lett. **74**, 2447 (1995).
[3] Y.-Q. Li and M. Xiao, Opt. Lett. **21**, 1064 (1996).
[4] B. S. Ham, M. S. Shahriar, and P. R. Hemmer, Opt. Lett. **22**, 1138 (1997).
[5] S. E. Harris and M. Jain, Opt. Lett. **22**, 636 (1997).
[6] G. Z. Zhang, D. W. Tokaryk, B. P. Stoicheff, and K. Hakuta, Phys. Rev. A **56**, 813 (1997).
[7] R. M. Whitley and C. R. Stroud, Jr., Phys. Rev. A **14**, 1498 (1976).
[8] J. Gea-Banacloche, Y.-Q. Li, S.-Z. Jin, and M. Xiao, Phys. Rev. A **51**, 576 (1995).
[9] S. Shepherd, D. J. Fulton, and M. H. Dunn, Phys. Rev. A **54**, 5394 (1996).
[10] A. Kuhn, S. Steuerwald, and K. Bergman, Eur. J. Phys. **1**, 57 (1998).
[11] A. S. Zibrov, M. D. Lukin, D. E. Nikonov, L. Hollberg, M. O. Scully, V. L. Velichansky, and H. G. Robinson, Phys. Rev. Lett. **75**, 1499 (1995).
[12] R. R. Moseley, S. Shepherd, D. J. Fulton, B. D. Sinclair, and M. H. Dunn, Phys. Rev. Lett. **74**, 670 (1995).
[13] M. Jain, A. J. Merriam, A. Kasapi, G. Y. Yin, and S. E. Harris, Phys. Rev. Lett. **75**, 4385 (1995).